Interface-roughening phase diagram of the three-dimensional Ising model for all interaction anisotropies from hard-spin mean-field theory

Tolga Çağlar[1,2] and A. Nihat Berker[1,3]
[1]*Faculty of Engineering and Natural Sciences, Sabancı University, Orhanlı, Tuzla 34956, Istanbul, Turkey*
[2]*Department of Physics, Koç University, Sarıyer 34450, Istanbul, Turkey*
[3]*Department of Physics, Massachusetts Institute of Technology, Cambridge, Massachusetts 02139, USA*
(Received 24 September 2011; published 28 November 2011)

The roughening phase diagram of the $d = 3$ Ising model with uniaxially anisotropic interactions is calculated for the entire range of anisotropy, from decoupled planes to the isotropic model to the solid-on-solid model, using hard-spin mean-field theory. The phase diagram contains the line of ordering phase transitions and, at lower temperatures, the line of roughening phase transitions, where the interface between ordered domains roughens. Upon increasing the anisotropy, roughening transition temperatures settle after the isotropic case, whereas the ordering transition temperature increases to infinity. The calculation is repeated for the $d = 2$ Ising model for the full range of anisotropy, yielding no roughening transition.

DOI: 10.1103/PhysRevE.84.051129 PACS number(s): 05.50.+q, 68.35.Ct, 64.60.De, 75.60.Ch

I. INTRODUCTION

The ordering phase transition in a crystal precipitates the formation of macroscopic domains, differently ordered with respect to each other. The interface between such domains incorporates static and dynamic phenomena of fundamental and applied importance. Of singular importance is the occurrence of yet another phase transition, distinct from the ordering phase transition, which is the interface roughening phase transition [1,2]. The roughening phase transition is well studied with the three-dimensional Ising model, in the so-called solid-on-solid limit, in which the interactions along one spatial direction (z) are taken to infinite strength, while the interactions along the x and y spatial directions remain finite. In this case, due to the infinite interactions, the ordering phase transition moves to infinite temperature and is not observed. A study of the system with finite interactions, where both ordering and roughening phase transitions should distinctly be observed, had not been done.

In our current study, hard-spin mean-field theory [3,4], which has been qualitatively and quantitatively successful in frustrated and unfrustrated magnetic ordering problems [3–18], is used to study ordering and roughening phase transitions in the three-dimensional ($d = 3$) Ising model for the entire range of interaction anisotropies, continuously from the solid-on-solid limit to the isotropic system to the weakly coupled-planes limit. The phase diagram is obtained in the temperature and interaction anisotropy variables, with separate curves of ordering and roughening phase boundaries. The method, when applied to the anisotropic $d = 2$ Ising model, yields the lack of roughening phase transition.

II. HARD-SPIN MEAN-FIELD THEORY

Hard-spin mean-field theory has been introduced as a self-consistent theory that conserves the hard-spin ($|s| = 1$) condition, indispensable to the study of frustrated systems [3,4]. This method is almost as simply implemented as usual mean-field theory, but brings considerable qualitative and quantitative improvements. Hard-spin mean-field theory has yielded, for example, the lack of order in the undiluted zero-field triangular-lattice antiferromagnetic Ising model and the ordering that occurs either when a uniform magnetic field is applied to the system, giving a quantitatively accurate phase diagram in the temperature versus magnetic field variables [3–6,9,10], or when the system is sublattice-wise quench-diluted [17]. Hard-spin mean-field theory has also been successfully applied to complicated systems that exhibit a variety of ordering behaviors, such as three-dimensionally stacked frustrated systems [3,7], higher-spin systems [8], and hysteretic $d = 3$ spin glasses [18]. Furthermore, hard-spin mean-field theory shows qualitative and quantitative effectiveness for unfrustrated systems as well, such as being dimensionally discriminating by yielding the no-transition of $d = 1$ and improved transition temperatures in $d = 2$ and 3 [5,18].

We have therefore applied hard-spin mean-field theory to the global study of the roughening transition in the anisotropic $d = 3$ Ising model. [We have also found that no roughening phase transition is seen in $d = 2$ (Sec. IV).] The uniaxially anisotropic $d = 3$ Ising model is defined by the Hamiltonian

$$-\beta\mathcal{H} = J_{xy}\sum_{\langle ij\rangle}^{xy} s_i s_j + J_z \sum_{\langle ij\rangle}^{z} s_i s_j, \qquad (1)$$

where, at each site i of a $d = 3$ cubic lattice with periodic boundary conditions, $s_i = \pm 1$. The first sum is over nearest-neighbor pairs of sites along the x and y spatial directions, and the second sum is over the nearest-neighbor pairs of sites along the z spatial direction. The interactions are ferromagnetic, $J_{xy}, J_z > 0$, except for the interaction between two of the xy planes, which has the same magnitude as the other J_z interactions but is antiferromagnetic: $J_z^A = -J_z < 0$. This choice is made in order to induce an interface when the system is ordered. (An alternate approach would have been to use a system without periodic boundary conditions along the z direction, but with oppositely pinned spins at each edge. However, this would have introduced a surface effect at the pinned edges, modifying the magnetization deviations which would thereby not exclusively reflect the spreading of the interface.)

For this system, the self-consistent equation of hard-spin mean-field theory is

$$m_i = \sum_{\{s_j\}} \left[\left(\prod_j P(m_j, s_j) \right) \tanh \left(\sum_j J_{ij} s_j \right) \right], \qquad (2)$$

where the last sum is over the sites j that are nearest neighbor to site i, and the first sum is over all states $\{s_j\}$ of the spins at these nearest-neighbor sites. In Eq. (2),

$$P(m_j, s_j) = \tfrac{1}{2}(1 + m_j s_j) \qquad (3)$$

is, for local magnetization m_j at site j, the probability of having the spin value of s_j. The coupled Eqs. (2) are solved numerically for a $20 \times 20 \times 20$ cubic system with periodic boundary conditions, by iteration: A set of magnetizations is substituted into the right-hand side of Eqs. (2), to obtain a new set of magnetizations from the left-hand side. This new set is then substituted into the right-hand side, and this procedure is carried out repeatedly, converging to stable values of the magnetizations that are the solution of the equations. The resulting magnetization values depend on the z coordinate only.

III. RESULTS: ORDERING AND ROUGHENING PHASE TRANSITIONS IN $d = 3$

A series of curves for the magnetizations m_i versus xy layer number i are shown for different temperatures $1/J_{xy}$, for a given anisotropy J_z/J_{xy} in each panel of Fig. 1. For each value of the anisotropy, the magnetizations m_i are zero at high temperatures and become nonzero below the ordering transition temperature T_C. The ordering onset is seen in the upper panel of Fig. 2, where the magnetization absolute values $|m_b|$ away from the interface are plotted as a function of temperature $1/J_{xy}$, for different values of the anisotropy J_z/J_{xy}.

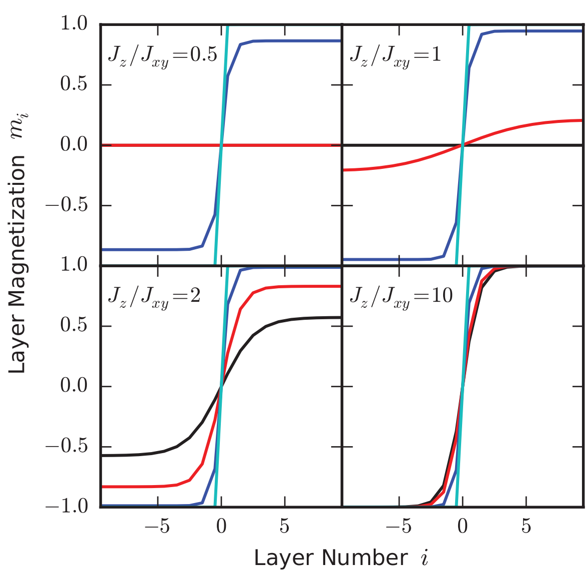

FIG. 1. (Color online) For the $d = 3$ anisotropic Ising model, magnetizations m_i versus xy layer-number i curves for different temperatures $1/J_{xy}$. Each panel shows results for the indicated anisotropy J_z/J_{xy}. The curves in each panel, with decreasing sharpness, are for temperatures $1/J_{xy} = 1,\ 3,\ 5,\ 6$. In the upper panels, the high-temperature curves coincide with the horizontal line $m_i = 0$.

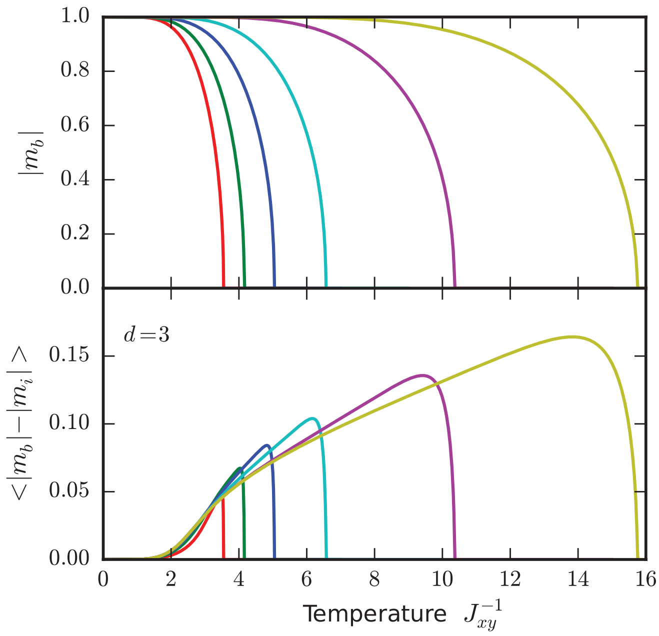

FIG. 2. (Color online) Local magnetization data for the $d = 3$ anisotropic Ising model. The curves, starting from the high-temperature side, are for anisotropies $J_z/J_{xy} = 10,\ 5,\ 2,\ 1,\ 0.5,\ 0.2$. Upper panel: Magnetization absolute values $|m_b|$ away from the interface as a function of temperature $1/J_{xy}$, for different values of the anisotropy J_z/J_{xy}. Lower panel: The deviation $|m_b| - |m_i|$ averaged over the system versus temperature $1/J_{xy}$ for different anisotropies J_z/J_{xy}. This averaged deviation vanishes when the interface is smooth. Note the qualitatively different low-temperature behavior in the $d = 2$ case shown in Fig. 4.

In Fig. 1, it is also seen that, at temperatures just below T_C, the interface between the $m_i \gtrless 0$ domains is spread over several layers. It is also seen that below a lower, roughening-transition temperature T_R, the interface becomes localized between two consecutive layers, reversing the sign of the magnetization m_i with no change in magnitude. This onset is best seen in the lower panel of Fig. 2, where the deviation $|m_b| - |m_i|$ averaged over the system is plotted as a function of temperature $1/J_{xy}$ for different anisotropies J_z/J_{xy}.

Thus, we have deduced the phase diagram, for all values of the anisotropy J_z/J_{xy} and temperature $1/J_{xy}$, as shown in Fig. 3. The roughening transition is obtained by fitting the averaged deviation curves (lower panel of Fig. 2) within the range $\langle |m_b| - |m_i| \rangle = 0.01$ to 0.04, to find the temperature at which the averaged deviation reaches zero, meaning that the interface becomes localized between two consecutive layers, reversing the sign of the magnetization m_b with no change in magnitude. In Fig. 3 the ordering and roughening phase transitions occur as two separate curves, starting in the decoupled planes ($J_z/J_{xy} = 0$) limit and scanning at finite temperature the entire range of anisotropies. The ordering transition starts, for the decoupled planes limit $J_z/J_{xy} = 0$, at $1/J_{xy} = 3.12$, to be compared with the exact result of $1/J_{xy} = 2.27$. The ordering transition continues to $1/J_{xy} = 5.06$, to be compared with the precise [19] result of $1/J_{xy} = 4.51$,

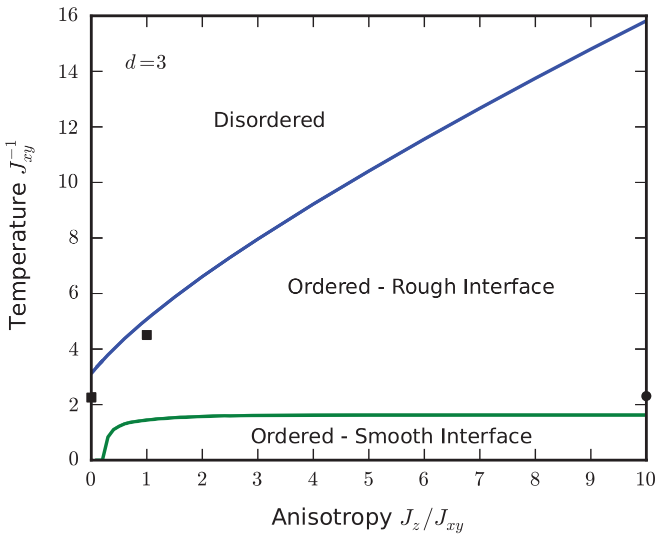

FIG. 3. (Color online) For the $d = 3$ anisotropic Ising model, the calculated phase diagram showing the disordered, ordered with rough interface, and ordered with smooth interface phases. The squares indicate the exact ordering temperatures from duality at $J_z/J_{xy} = 0$ and from Ref. [19] at $J_z/J_{xy} = 1$. The circle indicates the roughening transition temperature for the solid-on-solid limit $J_z/J_{xy} \to \infty$ [2]. The roughening transition is obtained by fitting the averaged deviation curves (lower panel of Fig. 2) within the range $\langle |m_b| - |m_i| \rangle = 0.01$ to 0.04, to find the temperature at which the averaged deviation reaches zero, meaning that the interface becomes localized between two consecutive layers, reversing the sign of the magnetization m_b with no change in magnitude.

for the isotropic case $J_z/J_{xy} = 1$. In the solid-on-solid limit ($J_z/J_{xy} \to \infty$), the ordering boundary goes to infinite temperature. The roughening transition starts at $1/J_{xy} = 0$ for J_z/J_{xy} close to zero and settles to a finite temperature value before the isotropic case. Thus, the roughening transition temperature $1/J_{xy}$ is 1.45 in the isotropic case $J_z/J_{xy} = 1$ and 1.62 in the solid-on-solid limit $J_z/J_{xy} \to \infty$, the latter to be compared with the value of 2.30 ± 0.10 from Ref. [2].

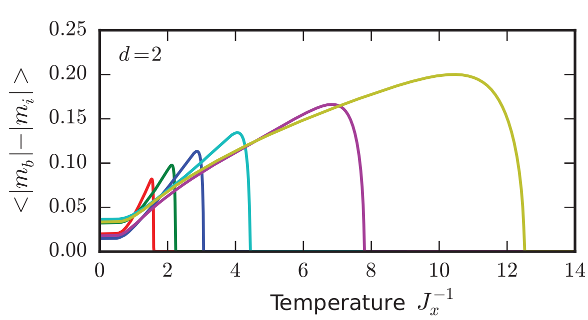

FIG. 4. (Color online) For the $d = 2$ anisotropic Ising model, the deviation $|m_b| - |m_i|$ averaged over the system versus temperature $1/J_{xy}$ for different anisotropies J_z/J_{xy}. The curves, starting from the high-temperature side, are for anisotropies $J_z/J_{xy} = 10,\ 5,\ 2,\ 1,\ 0.5,\ 0.2$. It is seen that the deviation does not vanish, i.e., the interface does not localize, down to zero temperature. Thus, a qualitatively different low-temperature behavior occurs, as compared with the $d = 3$ case shown in the lower panel of Fig. 2.

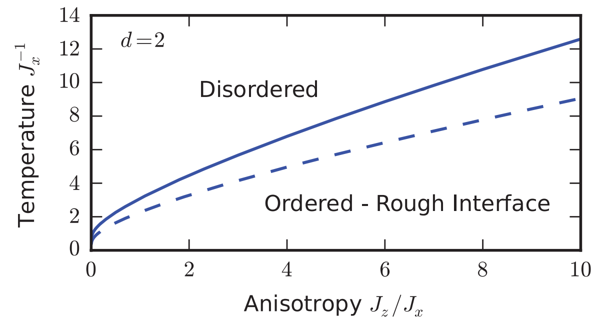

FIG. 5. (Color online) For the $d = 2$ anisotropic Ising model, the phase diagram showing the disordered phase and the ordered phase with rough interface. The dashed curve is the exact ordering boundary $\sinh(2J_x)\sinh(2J_z) = 1$ obtained from duality. No ordered phase with smooth interface is found.

IV. RESULTS: ORDERING TRANSITIONS BUT NO ROUGHENING TRANSITIONS IN $d = 2$

We have also applied our method to the anisotropic $d = 2$ Ising model, defined by the Hamiltonian

$$-\beta\mathcal{H} = J_x \sum_{\langle ij \rangle}^{x} s_i s_j + J_z \sum_{\langle ij \rangle}^{z} s_i s_j, \quad (4)$$

where, on a 20×20 square lattice with periodic boundary conditions, the first sum is over nearest-neighbor pairs of sites along the x spatial direction, and the second sum is over the nearest-neighbor pairs of sites along the only other (z) spatial direction.

The ordering phase transition is observed in $d = 2$ similarly to the $d = 3$ case. However, the rough interface phase continues to zero temperature, as seen in the $|m_b| - |m_i|$ curves in Fig. 4. Thus, no roughening phase transition occurs in $d = 2$. The corresponding phase diagram is given in Fig. 5. The ordering transition starts, for the decoupled lines limit $J_z/J_x = 0$, at $1/J_x = 0$, as expected for decoupled $d = 1$ systems. The ordering transition continues to $1/J_x$ =3.09, to be compared with the exact result of $1/J_x = 2.27$, for the isotropic case $J_z/J_x = 1$. In the $J_z/J_x \to \infty$ limit, the ordering boundary goes to infinite temperature.

V. CONCLUSION

It seen that hard-spin mean-field theory yields a complete picture of the ordering and roughening phase transitions for the isotropic and anisotropic Ising models, in spatial dimensions $d = 3$ and 2. This result attests to the microscopic efficacy of the model. Future works, such as the effects of uncorrelated and correlated (aerogel [20,21]) frozen impurities on the roughening transitions, are planned.

ACKNOWLEDGMENTS

Support by the Alexander von Humboldt Foundation, the Scientific and Technological Research Council of Turkey (TÜBİTAK), and the Academy of Sciences of Turkey is gratefully acknowledged.

[1] S. T. Chui and J. D. Weeks, Phys. Rev. **14**, 4978 (1976).
[2] R. H. Swendsen, Phys. Rev. B **15**, 5421 (1977).
[3] R. R. Netz and A. N. Berker, Phys. Rev. Lett. **66**, 377 (1991).
[4] R. R. Netz and A. N. Berker, J. Appl. Phys. **70**, 6074 (1991).
[5] J. R. Banavar, M. Cieplak, and A. Maritan, Phys. Rev. Lett. **67**, 1807 (1991).
[6] R. R. Netz and A. N. Berker, Phys. Rev. Lett. **67**, 1808 (1991).
[7] R. R. Netz, Phys. Rev. B **46**, 1209 (1992).
[8] R. R. Netz, Phys. Rev. B **48**, 16113 (1993).
[9] A. N. Berker, A. Kabakçıoğlu, R. R. Netz, and M. C. Yalabık, Turk. J. Phys. **18**, 354 (1994).
[10] A. Kabakçıoğlu, A. N. Berker, and M. C. Yalabık, Phys. Rev. E **49**, 2680 (1994).
[11] E. A. Ames and S. R. McKay, J. Appl. Phys. **76**, 6197 (1994).
[12] G. B. Akgüç and M. Cemal Yalabık, Phys. Rev. E **51**, 2636 (1995).
[13] J. E. Tesiero and S. R. McKay, J. Appl. Phys. **79**, 6146 (1996).
[14] J. L. Monroe, Phys. Lett. A **230**, 111 (1997).
[15] A. Pelizzola and M. Pretti, Phys. Rev. B **60**, 10134 (1999).
[16] A. Kabakçıoğlu, Phys. Rev. E **61**, 3366 (2000).
[17] H. Kaya and A. N. Berker, Phys. Rev. E **62**, R1469 (2000); also see M. D. Robinson, D. P. Feldman, and S. R. McKay, Chaos **21**, 037114 (2011).
[18] B. Yücesoy and A. N. Berker, Phys. Rev. B **76**, 014417 (2007).
[19] A. M. Ferrenberg and D. P. Landau, Phys. Rev. B **44**, 5081 (1991).
[20] S. B. Kim, J. Ma, and M. H. W. Chan, Phys. Rev. Lett. **71**, 2268 (1993).
[21] A. Falicov and A. N. Berker, Phys. Rev. Lett. **74**, 426 (1995).